INEEL/CON-99-01026
PREPRINT

A Technique for Dynamic Corrosion Testing in Liquid Lead Alloys

E. P. Loewen
C. B. Davis
P. E. MacDonald

April 2, 2000 – April 6, 2000

8th International Conference on Nuclear Engineering

BECHTEL BWXT IDAHO, LLC

A TECHNIQUE FOR DYNAMIC CORROSION TESTING IN LIQUID LEAD ALLOYS

Eric P. Loewen
Bechtel BWXT Idaho, LLC
Idaho National Engineering and Environmental Laboratory
P.O. Box 1625
Idaho Falls, Idaho 83415-3860
USA
(208) 526-9404
(208) 526-2930 (fax)
loewep@inel.gov

Cliff B. Davis
Bechtel BWXT Idaho, LLC
Idaho National Engineering and Environmental Laboratory
P.O. Box 1625
Idaho Falls, Idaho 83415-3890
USA
(208) 526-9470
(208) 526-6971 (fax)
cbd@inel.gov

Philip E. MacDonald
Bechtel BWXT Idaho, LLC
Idaho National Engineering and Environmental Laboratory
P.O. Box 1625
Idaho Falls, Idaho 83415-3870
USA
(208) 526-9634
(208) 526-2930 (fax)
pem@inel.gov

Keywords: Lead, Lead–bismuth, Corrosion, ATHENA, Fast Reactor

ABSTRACT

An experimental apparatus for the investigation of the flow-assisted dissolution and precipitation (corrosion) of potential fuel cladding and structural materials to be used in liquid lead alloy cooled reactors has been designed. This experimental project is part of a larger research effort between Idaho National Engineering and Environmental Laboratory (INEEL) and Massachusetts Institute of Technology to investigate the suitability of lead, lead-bismuth, and other lead alloys for cooling fast reactors designed to produce low-cost electricity as well as for actinide burning.

The INEEL forced convection corrosion cell consists of a small heated vessel with a shroud and gas flow system. The gas flow rates, heat input, and shroud and vessel dimensions have been adjusted so that a controlled coolant flow rate, temperature, and oxygen potential are created within the downcomer located between the shroud and vessel wall. The ATHENA computer code was used to design the experimental apparatus and estimate the fluid conditions. The corrosion cell will test steel that is commercially available in the U. S. to temperatures above 650°C.

INTRODUCTION

This experimental project is part of a larger University Research Collaboration program at the INEEL to investigate the suitability of lead-bismuth cooled fast reactors for producing low-cost electricity as well as for actinide burning. The goal is to identify and analyze the key technical issues in core neutronics, materials, thermal-hydraulics, fuels, and economics associated with the development of this reactor concept. This project is focused on materials testing; specifically corrosion tests with molten lead (Pb) alloys.

Lead-bismuth coolant systems have been used in Russian submarines (Adamov and Orlov, 1997; Gromov et al., 1994; and Kuznetsov and Sekimoto, 1995) and submarine prototype reactors for a number of years. Los Alamos National Laboratory (LANL) is investigating the use of molten lead-bismuth coolant for their accelerator-driven sub-critical pile to burn actinides. This research has been undertaken to evaluate the corrosion of potential fuel cladding and structural materials, which are compatible with molten Pb-alloys. This initial work is to provide the INEEL with experience in handling molten Pb-alloys, understanding their interaction with other metals (validating the Russian research), and adding to the knowledge base (supporting the development at LANL and elsewhere).

Considerable work in the field of molten Pb liquid-metal corrosion was undertaken in the 1950's (Brasunas and Manly, 1954; Cathcart, 1952; Cathcart and Manly, 1954; Clifford, 1960; and Romano et al., 1963). Much of the effort with Pb-alloys was discontinued once liquid sodium was selected as the liquid metal coolant for the second U.S. Naval submarine, and for the EBR-I and EBR-II reactors. Sodium was selected because its use resulted in a better doubling time and lead alloys, at the temperatures of interest, were corrosive to structural materials. The shorter doubling time of sodium cooled reactors is of little significance today as we do not foresee a depletion of low cost uranium resources in the near future and we have a significant inventory of actinides which can be burned in a fast reactor. Lead-bismuth liquid-metal corrosion of structural steels is mainly dependent on the solubility rate of the structural material in the liquid metal. The solubility rate is affected by diffusion barriers, metal oxides, nitrides, and other surface compounds; and by impurities in both the molten Pb alloy and structural metal. Mass transfer may occur in these systems (due to isothermal mass transfer caused by composition gradients, thermal-gradient mass transfer, and energy-gradient mass transfer) causing reorientation of surface contours to one of a lower energy state (Brasunas and Manly, 1954).

The reason for the current interest in liquid Pb-alloys for reactor cooling is because of their excellent physical characteristics. For example, Pb-alloys have a high thermal conductivity and are chemically inert with air and water. The boiling point of Pb-alloys is high, allowing low-pressure operation at high temperatures. Also, the harder neutron spectrum of a lead-bismuth reactor provides improved neutron economy. Some disadvantages of Pb-alloys are melting points above room temperature, material compatibility issues, and handling and containment issues. The latter include instrumentation and maintenance issues since all pipes carrying Pb-alloys must be provided with heaters to prevent solidification in case of reactor shutdown.

Relative to the material compatibility issues, it was found that nickel and nickel-containing alloys, such as the austenitic steels, are unsatisfactory container materials for liquid Pb-alloys at temperatures above 500^{o}C (Brasunas and Manly, 1952; Cathcart, 1952; Clifford, 1960; Romano et al., 1963). This is attributed to the preferential solution of nickel and iron from these materials and the precipitation of the material in colder regions of the system. Although this is not an electrochemical process, we use the word corrosion is this paper to describe it. For ferritic steels, increased chromium content seems to increase corrosion resistance due possibly to the formation of chrome and/or iron chrome oxides that protect the steel from attack. Static tests conducted with these steels indicate that increasing the chromium content increases the corrosion resistance at temperatures below 650^{o}C (Everhart and Van Nuis, 1950). The trend is reversed above 750^{o}C and the low chromium steels are more resistant. Mild carbon steels suffer moderate penetration in static tests and their usefulness in a flow system is probably limited to temperatures below 450^{o}C. The Russians have found that steels with relatively low levels of nickel (0.8%) and relatively high levels of silicon (1.3%) and vanadium (0.4%) seem to work well in contact with molten Pb-alloys at temperatures up to about 600°C.

The overall objectives of this current research are to:

1) Deploy Pb-alloy corrosion cells at the INEEL to carry out an independent investigation of the corrosion of potential fuel cladding and reactor structural materials exposed to molten Pb-alloys. This corrosion tester will be built from materials that are commercially available.
2) Develop O_2 probes that will measure the oxygen concentration in the molten Pb-alloys.
3) Discover what measures have to be taken to ensure the re-formation of the protective oxide film of structural materials.
4) Obtain corrosion data on different Pb-alloy systems, for example Pb, Pb-Bi, Pb-Sn, etc.
5) Develop an oxidation/reduction control system to provide a protective layer to structural material.

DESIGN

An experimental unit is being built at INEEL to test dynamic corrosion in an environment that approaches the conditions that would be present in a nuclear reactor core. The oxide layer on the metal components will be controlled in the belief that it will provide a protective coating, thereby limiting corrosion. Figure 1 shows the free energy of formation of typical oxides in this system. Notice that the Pb and Bi oxides are less favorable than the chrome and iron oxides. Therefore, we will use a sealed corrosion cell that will be heated with a resistance coil to control the formation of the oxide layer on the structural material.

An overall diagram of the experimental apparatus is provided in Fig. 2. A resistance furnace used in previous fusion corrosion tests will heat the Pb-alloy. Heating will be controlled by K-type thermocouples. Process gas will be supplied from standard high-pressure gas bottles. Venting of the experimental system will be through cooled media to ensure that no Pb vapor escapes to the environment. The corrosion cell will be contained in a stainless steel can. Each of the experimental sub-systems are described below:

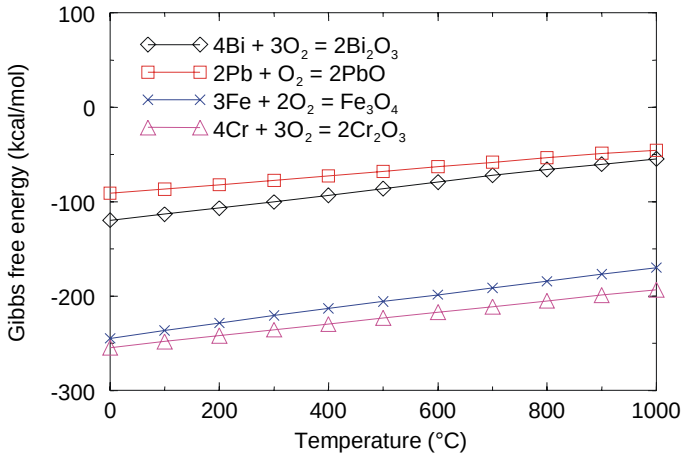

Fig.1. Gibbs free energy of formation of typical oxides.

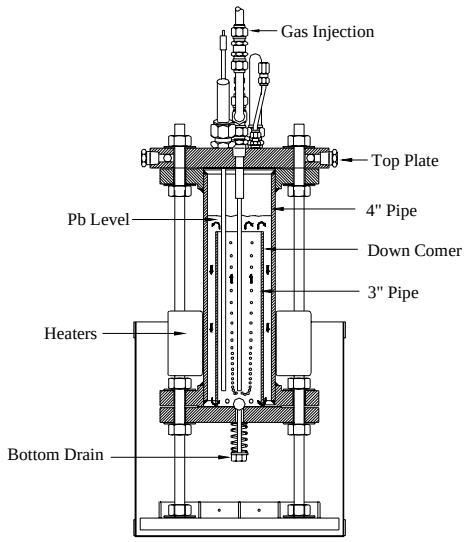

Fig. 2. Experimental apparatus.

1) Gas Injection System: Two pressure-regulated manifolds will deliver an inert gas (Ar, He, or N_2) into the corrosion vessel. The gas injection will occur above and below the liquid metal. The anticipated gas flow rate is about 30 standard liters per minute. O_2 can be added to the inert gas injected below the surface of the molten Pb-alloy to oxidize it. The O_2 source will come from a standard gas cylinder with O_2 added into an inert gas carrier (He, Ar, N_2). A reducing agent (H_2) will be injected into the corrosion cell headspace to remove metal oxides and control O_2 levels in the corrosion cell.
2) Corrosion Cell: This cell will be constructed from standard pipe with welded on flanges. The cell will have several gas-tight fittings on top to allow gas injection, off-gas removal, and temperature and O_2 measurement. The pipe (initially containing a solidified Pb-alloy) will be located in a small (18 cm diameter) electric furnace. The electric furnace, utilizing standard heating equipment, will heat the pipe and, in turn, melt the Pb-alloy sealed within. Cooling coils can be soldered to the exterior of the upper pipe wall to increase the thermal gradient between the hot and cold regions in the cell.
3) Gas Handling System: This system takes the off-gas from the corrosion cell, cools it, filters it and captures dust before discharging it into the suction of a HEPA-AIRE portable air scrubber system which consists of pre-filter, activated carbon filter, second stage filter and then a HEPA filter.
4) Specialized Ventilation: The experimental unit will use a portable HEPA system. The unit is powered by 110 VAC, is on wheels, has a variable flow rate, and has three media for filtration (pre-filter, carbon filter, and HEPA filter).

The corrosion cell contains a small vessel, with an inner diameter of approximately 10.2-cm, that is separated into three regions by a shroud. The three regions include a riser that is located inside the shroud, a downcomer that is located between the shroud and the vessel wall, and an upper plenum region located above the top of the shroud. The experiment will contain a pool of a molten Pb-alloy with a level above the top of the shroud. An inert gas will be injected into the riser near its bottom. The inert gas will flow up through the riser, reducing the hydrostatic head in the riser. The difference in hydrostatic head between the riser and downcomer will then cause liquid lead to flow up through the riser, down the downcomer, and back to the riser through a gap located at the bottom of the shroud. The inert gas will separate in the upper plenum and be removed through the top of the vessel. Varying the flow through the downcomer will allow us to evaluate the effects of flow on erosion. The cell gas injection system has the capability to inject both oxidative (CO_2 and O_2) and reducing gases (H_2). This will allow us to control the oxidative potential in the cell as was previously shown in Fig. 1. The reductive and oxidative gas will make up a small part of the gas injected into the bottom of the riser. The fluid velocity in the downcomer will be controlled by adjusting the gas flow. The oxidation potential will be corrected as needed.

Table 1 presents a summary of the planned experimental parameters.

Table 1. Experimental test matrix.

Metal	Temperature (°C)	Time (hours)	Alloy
Fe	450	6	Pb
Fe	550-650	24	Pb-Bi
316 Stainless	650	24	Pb
Fe	550	100	Pb
Fe	650	100	Pb-Bi
316 Stainless	550	100	Pb-Bi
316 Stainless	650	100	Pb-Bi
410 Stainless	550	100	Pb-Bi
316 Stainless	650	100	Pb
410 Stainless	550	100	Pb
410 Stainless	650	100	Pb-Bi
Zr w/ 2 % Nb	550	100	Pb-Bi
Zr w/ 2 % Nb	650	100	Pb

FLOW CALCULATIONS

The ATHENA computer code (Carlson et al., 1986) was used in the hydraulic design of the corrosion experiment. The ATHENA code is incorporated as a compile time option in the RELAP5-3Dχ computer code (the RELAP5-3D Development Team, 1999), which in turn is an extension of RELAP5/MOD3 (the RELAP5 Development Team, 1995). The principal difference between RELAP5 and ATHENA is that RELAP5 was designed to use water as the working fluid while ATHENA allows the use of many different working fluids, including lead-bismuth. The Pb-alloy was assumed to be lead-bismuth in these initial calculations. The code was modified to use the El-Boher and Lesin void correlation (1988) in the riser and upper plenum regions. The El-Boher and Lesin correlation was developed to describe the void fraction during co-current, upward flow in a pipe for several two-phase fluids, including a mixture of lead-bismuth and steam.

An ATHENA input model of the corrosion experiment was developed as illustrated in Fig. 3. The model represents the riser, upper plenum, and downcomer regions. The riser was represented with nine control volumes. The lowest control volume represented the gap at the bottom of the shroud and was 1.27 cm tall. The remainder of the riser was divided equally into eight control volumes. The liquid level was initialized 2.54 cm above the top of the shroud, corresponding to the bottom of component 550. A time-dependent junction (component 515) was used to inject gas into the riser. A time-dependent volume (component 560) was used to set the pressure of the system and to receive the gas injected into the riser.

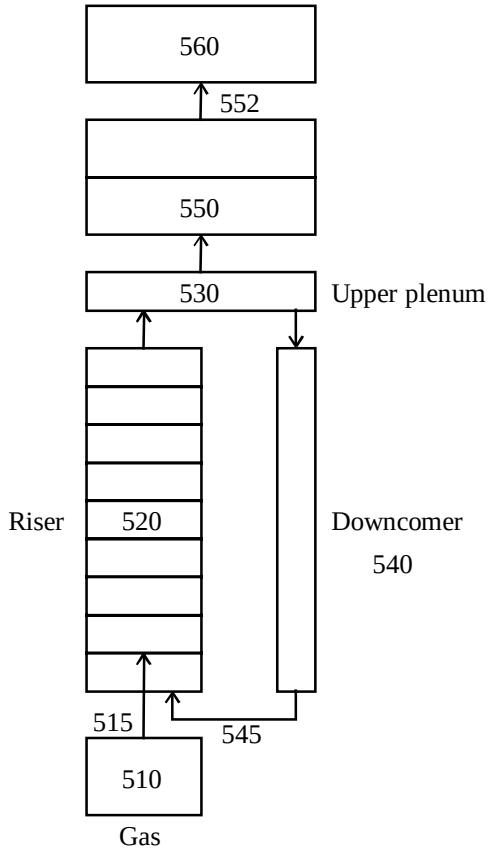

Fig. 3. Nodalization of the ATHENA input model.

A series of calculations was performed to determine the shroud diameter that maximizes the fluid velocity in the downcomer. These calculations were performed at a system pressure of $1x10^5$ Pa, an isothermal temperature of 450°C, and a gas flow rate of 0.0006 kg/s. The shroud height and thickness were assumed to be 27.9 and 0.305 cm, respectively. The gas was assumed to be air.

The effect of the shroud inner diameter on the fluid velocity in the downcomer is presented in Fig. 4. The figure shows that the maximum downcomer fluid velocity occurred when the shroud inner diameter was about 8.1 cm. The maximum in velocity occurs because of two competing effects. The first effect is simply that due to the influence of the flow area on the fluid velocity at a constant flow rate. As the shroud diameter decreases, the downcomer flow area increases and the velocity decreases in order for the flow rate to remain constant. The second effect is that due to the influence of the downcomer hydraulic diameter and flow area on the frictional pressure drop around the flow circuit. The major hydraulic losses in the test loop are due to wall friction in the downcomer and form losses at the top and bottom of the downcomer. The hydraulic resistance of the riser is relatively small. As the shroud diameter decreases, the downcomer flow area and hydraulic diameter increase, which decreases the frictional pressure drop

across the downcomer and causes an increase in the natural circulation flow rate, which tends to increase the fluid velocity in the downcomer. Fig. 4 indicates that the first effect is more important for shroud inner diameters less than 8.1 cm and that the second effect is more important at larger diameters. For example, as the inner diameter increased above 8.1 cm, the frictional pressure drop across the downcomer increased, causing the natural circulation flow rate to decrease. The effect of the smaller natural circulation flow rate more than offset the increase in velocity associated with the smaller area assuming a constant flow rate.

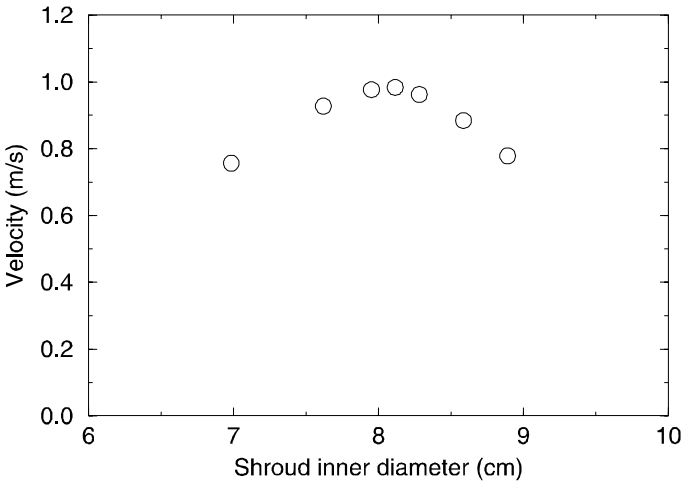

Fig.4. Downcomer velocity as a function of shroud diameter.

Based on the results shown in Fig. 4, 3-inch schedule-10S pipe was purchased to form the inner shroud. The inner diameter of this pipe (8.28 cm) is very close to the value that maximizes the fluid velocity in the downcomer.

Additional calculations were performed to determine the effect of gas flow rate on the fluid velocity in the downcomer. These calculations, which are summarized in Fig. 5, were performed with a shroud inner diameter of 8.28 cm and with two different shroud heights, 12.7 cm and 27.9 cm. The figure shows that the downcomer velocity increases with the gas flow rate. The increase in velocity is caused by the increase in void fraction in the riser (see Fig. 6) which results in an increase in the difference in hydrostatic head between the riser and downcomer and a corresponding increase in the natural circulation flow rate.

Figure 5 also shows that the fluid velocity in the downcomer increases with shroud height. Assuming constant fluid properties, the difference in the hydrostatic head between the downcomer and the riser and the head loss due to wall friction are both proportional to the shroud height. However, the head losses due to the form loss coefficients at the top and the bottom of the downcomer are independent of the shroud height. Thus, the downcomer velocity increases with shroud height because the head losses associated with the form loss coefficients are relatively smaller with the taller shroud.

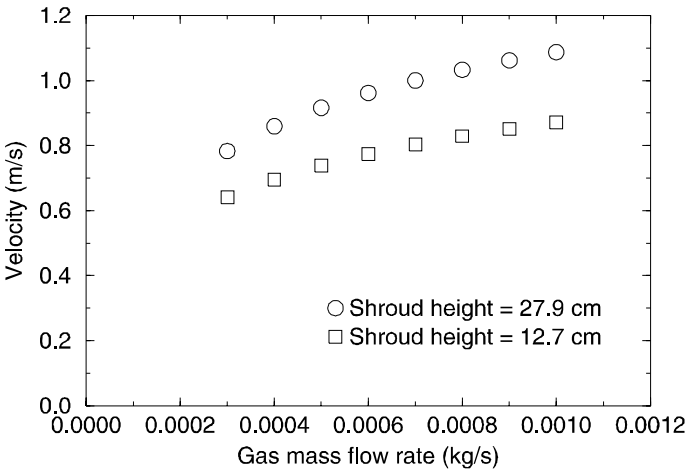

Fig. 5. Downcomer velocity as a function of gas flow rate.

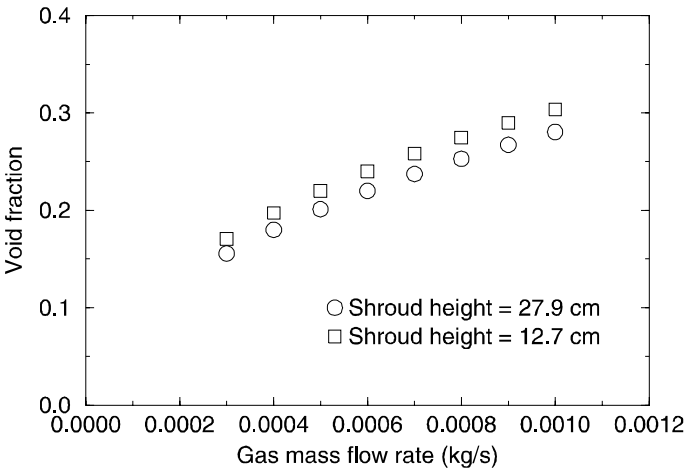

Fig. 6. Riser void fraction as a function of gas flow rate.

ATHENA predicted that gas was not entrained from the upper plenum into the downcomer for the gas flow rates shown in Fig. 5. However, gas entrainment was calculated when the gas flow rate exceeded 0.0012 kg/s. The capability of the code to calculate the onset of gas entrainment into the downcomer has not been assessed, nor has the ability of the code to predict the void fraction resulting from a co-current downward flow of a mixture of molten lead-bismuth and a non-condensable gas. Consequently, the possibility of gas entrainment into the downcomer introduces uncertainty into the flow calculations in excess of that normally expected.

THERMAL CALCULATIONS

The flow-assisted dissolution and precipitation processes in the corrosion cell will be affected by temperature differences between the hot and cold points in the system. Consequently, a series of ATHENA calculations was performed to estimate the temperature differences that could be obtained in this corrosion cell.

The ATHENA model illustrated in Fig. 3 was modified somewhat to perform these calculations. Specifically, additional control volumes were added to the downcomer and heat structures were added to represent the shroud and vessel wall. Heat was added to the lower 15.2 cm of the vessel wall to simulate the effects of the resistance heater. The cooling coils around the upper part of the vessel were simulated by water flowing upwards through an annulus around the outside of the upper vessel wall. The shroud height was assumed to be 27.9 cm.

Steady-state calculations were performed in which the heater power, cooling water flow rate and temperature, and gas flow rate were held constant until thermal equilibrium was reached. As expected, the system temperature changed until the power removed through the cooling coils balanced the power added by the heater.

Figure 7 shows the calculated fluid temperature in the riser as a function of heater power. The figure shows that a continuous power of about 34 kW yields a system temperature of 450°C, which is the minimum desired test temperature presented in Table 1. The maximum desired test temperature, 650°C, can be achieved using a heater power of about 59 kW.

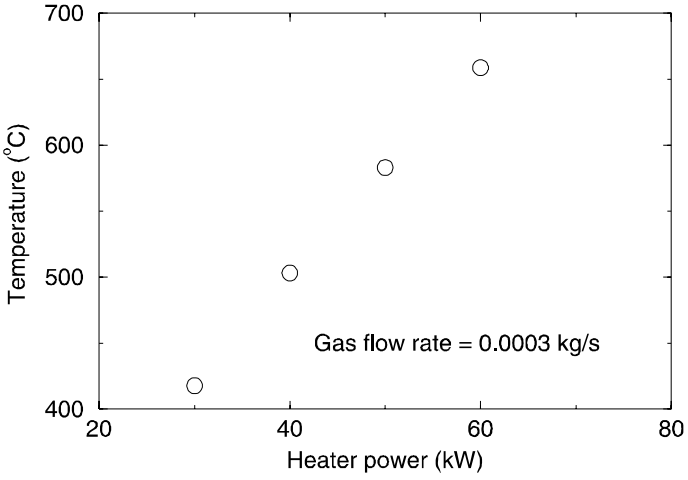

Fig. 7. System temperature as a function of heater power.

The calculated temperature difference between the hot and cold points in the flow circuit is shown in Fig. 8. The expected temperature difference in the corrosion cell varies from about 14°C at 34 kW to 22°C at 59 kW. These values are considerably less than those expected in a lead-bismuth cooled reactor, which vary from 50°C for a forced convection design to 300°C for a natural convection design (Buongiorno et al., 1999). Thus, it would be desirable to increase the temperature difference to make experimental results from the corrosion cell more applicable to a reactor. One way to increase the temperature difference would be to increase the height of the shroud, which would increase the heat transfer area available for cooling and would allow for an increased power while maintaining the system temperature at desired values. The temperature difference could also increased by changing the design to use an external loop in which the riser and downcomer sections could be heated and cooled independently.

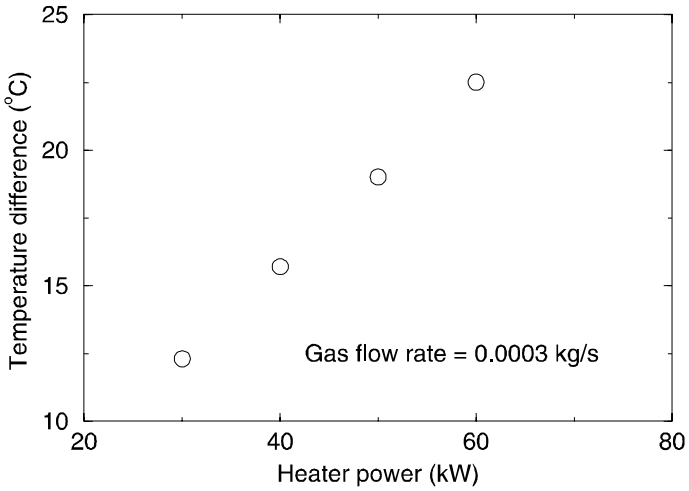

Fig. 8. Temperature difference as a function of heater power.

CONCLUSIONS

The INEEL is developing an experiment to study the effects of temperature, flow, and oxidation potential on the corrosion and erosion characteristics of typical structural materials that could be used in a nuclear power plant with molten lead-alloy coolant.

Flow calculations show that reasonable liquid velocities in the downcomer could be obtained with moderate gas flow rates.

Thermal calculations showed that the temperature difference between the hot and cold points in the corrosion cell is expected to be less than in current reactor designs. However, operation of the current design will provide valuable insights into the corrosion characteristics, operation, and control of lead-alloy systems. It is anticipated that the experimental design will be improved in the future to provide corrosion data at more typical conditions.

Future publications will provide experimental results.

ACKNOWLEDGMENT

Work supported through the INEEL Long-Term Research Initiative Program under DOE Idaho Operations Office Contract DE-AC07-99ID13727.

REFERENCES

Adamov, E. and Orlov, V., 1997, "Nuclear power at the next stage: cost-effective breeding, natural safety, radwastes, non-proliferation", Nuclear Engineering and Design 173, pp. 33-41.

Brasunas, A. and Manly, W. D., 1954, "Interim Report on Static Liquid-Metal Corrosion", ORNL 1647.

Buongiorno, J., et al., 1999, "Advanced Reactor Technology, Design of an Actinide Burning, Lead-Bismuth Cooled Reactor That Produces Low Cost Electricity, Annual Project Status Report," Idaho National Engineering and Environmental Laboratory, INEEL/EXT-99-00693, MIT-ANP-TR-065.

Carlson, K. E., Roth, P. A., and Ransom, V. H., 1986, "ATHENA Code Manual Vol. I: Code Structure, System Models, and Solution Methods," Idaho National Engineering Laboratory, EGG-RTH-7397.

Cathcart, J.V., 1952, "Mass Transfer in Dynamic Lead-Inconel Systems", ORNL 52-11-116.

Cathcart, J.V., and Manly, W. D., 1954, "A Technique for Corrosion Testing In Liquid Lead", ORNL 44960.

Clifford, J. C, 1960, "A Loop for Circulating Liquid Lead-Bismuth Mixtures: Corrosion Studies and Operation", Dissertation, Iowa State University of Science and Technology, Ames Iowa.

El-Boher, A., Lesin, S., Unger, Y., and Branover, H., 1988, "Experimental Studies of Liquid Metal Two-Phase Flows in Vertical Pipes," Proceedings of the 1st World Conference on Experimental Heat Transfer, Dubrovnik, Yugoslavia.

Everhart, J.L. and Van Nuis, E. L., 1950, "Liquid metal heat transfer fluid unstressed static corrosion tests." U.S. Atomic Energy Commission Report NP-1497.

Gromov, B.F., Belomyttsev, Y. S., Gubarev, V. A., Kalashnikov, A. G., Leonchuk, M. P., Novikova, N. N., Orlov, Y. U., 1994, "Inherently Safe Lead –Bismuth – Cooled Reactors. Atomic Energy, Vol. 76, No. 4.

Kuznetsov, V., and Sekimoto, H., 1995, "Radioactive Waste Transmutation and Safety Potentials for the Lead Cooled Fast Reactor in the Equilibrium State", Journal of Nuclear Science and Technology 32 6 pp. 507-516.

Romano, A.J., Klamut, C. J., and Gurinsky, D. H., 1963, "The Investigation of Container Materials for Bi and Pb Alloys Part I. Thermal Convection Loops", Brookhaven National Laboratory, BNL 811 (T-313).

The RELAP5-3Dχ Development Team, 1999, "RELAP5-3Dχ Code Manual Volume 1: Code Structure, System Models and Solution Methods," Idaho National Engineering and Environmental Laboratory, INEEL-EXT-98-00834.

The RELAP5 Development Team, 1995, "RELAP5/MOD3 Code Manual, Code Structure, System Models, and Solution Methods," Idaho National Engineering Laboratory, NUREG/CR-5535, INEL-95/0174, Volume 1.